



Contents lists available at ScienceDirect

Journal of Rock Mechanics and Geotechnical Engineering

journal homepage: www.rockgeotech.org

Review

Reliability of design approaches for axially loaded offshore piles and its consequences with respect to the North Sea

Kirill A. Schmoor^{a,*}, Martin Achmus^a, Aligi Foglia^b, Maik Wefer^b^a Institute for Geotechnical Engineering, Leibniz University Hannover, Hannover, 30167, Germany^b Fraunhofer Institute for Wind Energy Systems (IWES), Bremerhaven, 27572, Germany

ARTICLE INFO

Article history:

Received 27 September 2017

Received in revised form

13 April 2018

Accepted 5 June 2018

Available online xxx

Keywords:

Pile load test

Model error

System reliability

Global safety factors (GSFs)

Quality factors

ABSTRACT

In the near future, several offshore wind farms are planned to be built in the North Sea. Therefore, jacket and tripod constructions with mainly axially loaded piles are suitable as support structures. The current design of axial bearing resistance of these piles leads to deviant results regarding the pile resistance when different design methods are adopted. Hence, a strong deviation regarding the required pile length must be addressed. The reliability of a design method can be evaluated based on a model error which describes the quality of the considered design method by comparing measured and predicted pile bearing resistances. However, only few pile load tests are reported with regard to the boundary conditions in the North Sea. This paper presents 6 large-scale axial pile load tests which were incorporated within a new model error approach for the current design methods used for the axial bearing resistance, namely API Main Text method and cone penetration test (CPT)-based design methods, such as simplified ICP-05, offshore UWA-05, Fugro-05 and NGI-05 methods. Based on these new model errors, a reliability-based study towards the safety was conducted by performing a Monte-Carlo simulation. In addition, consequences regarding the deterministic pile design in terms of quality factors were evaluated. It is shown that the current global safety factor (GSF) prescribed and the partial safety factors are only valid for the API Main Text and the offshore UWA-05 design methods; whereas for the simplified ICP-05, Fugro-05 and NGI-05 design methods, an increase in the required embedded pile length and thus in the GSF up to 2.69, 2.95 and 3.27, respectively, should be considered to satisfy the desired safety level according to DIN EN 1990 of $\beta = 3.8$. Further, quality factors for each design method on the basis of all reliability-based design results were derived. Hence, evaluation of each design method regarding the reliability of the pile capacity prediction is possible.

© 2018 Institute of Rock and Soil Mechanics, Chinese Academy of Sciences. Production and hosting by Elsevier B.V. This is an open access article under the CC BY-NC-ND license (<http://creativecommons.org/licenses/by-nc-nd/4.0/>).

1. Introduction

In the near future, several offshore wind farms are planned to be built in the North Sea to satisfy the demand for a high amount of renewable energy in Germany. As most shallow-depth sea areas have already been exploited, a number of projects will be located in the sea areas with relatively large water depths (exceeding 40 m). For such water depths, jacket and tripod support structures with mainly axially loaded foundation piles will most probably be employed. Contrary to offshore oil and gas structures, offshore wind turbines are relatively light and dynamic-sensitive systems.

Therefore, the tension resistance of the piles is likely to be the design driver.

The axial bearing resistance of such piles is normally estimated according to the recommendation of API (2002) by applying the so-called “Main Text” method. However, several investigations have shown that the application of the Main Text method, at least for foundation piles of wind energy converters, is not reliable and may lead to a significant deviation compared to the in situ bearing capacity.

To enhance the reliability of design methods, 4 new cone penetration test (CPT)-based design methods, namely simplified ICP-05, offshore UWA-05, Fugro-05 and NGI-05, were introduced within API (2007). These methods were calibrated based on pile field tests, where basically the skin friction of a pile is estimated on the basis of the cone resistance of a CPT. Although it is believed that the proposed CPT-based methods are better than the API Main Text

* Corresponding author.

E-mail address: schmoor@igth.uni-hannover.de (K.A. Schmoor).

Peer review under responsibility of Institute of Rock and Soil Mechanics, Chinese Academy of Sciences.

<https://doi.org/10.1016/j.jrmge.2018.06.004>

1674-7755 © 2018 Institute of Rock and Soil Mechanics, Chinese Academy of Sciences. Production and hosting by Elsevier B.V. This is an open access article under the CC BY-NC-ND license (<http://creativecommons.org/licenses/by-nc-nd/4.0/>).

Please cite this article in press as: Schmoor KA, et al., Reliability of design approaches for axially loaded offshore piles and its consequences with respect to the North Sea, Journal of Rock Mechanics and Geotechnical Engineering (2018), <https://doi.org/10.1016/j.jrmge.2018.06.004>

method, care should be taken in the application of these methods since experience is limited. Instead, application of the CPT-based methods leads in practice to a high deviation in the required pile length within a design.

The accuracy of a design method can be described by a model error, which is usually defined as the ratio of the calculated bearing capacity to the measured or in situ bearing capacity of a pile according to Eq. (1). A model error close to unity indicates a reliable design method and vice versa. Often several results of measurements and predictions are taken into account, so that a distribution of the model error can be obtained. In this case, a model error with a mean value close to unity in combination with a low standard deviation indicates a suitable design method.

$$e_R = Q_c/Q_m \quad (1)$$

where Q_c is the calculated bearing capacity, and Q_m is the measured bearing capacity.

Compared to uncertainties arising from subsoil conditions such as inherent variability, statistical estimation errors and measurement errors, the model error represents the most dominant source of uncertainty with respect to the safety of a pile (Gilbert and Tang, 1995; Dithinde et al., 2011; Lacasse et al., 2013a). Consequently, if a reliability-based design is pursued, the model error should definitely be taken into account. However, it should be emphasized that the choice of the applied database strongly affects the model error (Lacasse et al., 2013b).

The aim of this study is to expand the existing database with respect to typical soil conditions and pile dimensions for axially loaded piles used in the North Sea by providing additional results from pile load tests. Six large-scale pile load tests were performed at the Test Center for Support Structures of the Leibniz University Hannover by the Fraunhofer Institute for Wind Energy Systems (IWES) within the IRPWind project. Considering these tests as well as the field load test results already published, a more precise model error approach for the existing design methods and assumed boundary conditions can be obtained.

In addition, for each design method, the corresponding failure probability as a function of the embedded pile length is determined by executing a Monte-Carlo simulation. Furthermore, the consequences regarding the deterministic design with respect to the obtained reliability-based results are discussed and evaluated.

2. Experimental program

2.1. Subsoil conditions

All experiments were conducted at the Test Centre for Support Structure of the Leibniz University Hannover by the Fraunhofer IWES. In this test facility, large-scale (1:10 to 1:5) geotechnical physical modeling can be performed by means of a 14 m long, 9 m wide and 10 m deep test pit which can be filled with granular material. Uniformly graded siliceous sand was used as soil medium. The grain size distribution and the essential properties of the soil are depicted in Fig. 1, where C_u is the coefficient of uniformity, C_c is the coefficient of curvature, G_s is the specific gravity of the soil, and n_{\min} and n_{\max} are respectively the minimum and maximum soil porosities.

The sand was prepared before the experimental campaign in a specific manner, which enabled the achievement of an excellent uniformity of the sand sample. For each sand layer, roughly 40 m³ of soil was poured into the test pit and equally distributed across the area to form a stratum of approximately 30 cm thick. Thereafter, single-direction plate compactors were employed over the previously laid soil layer which had a thickness of around 25 cm after compaction. The compaction state of each layer was investigated by carefully taking core samples across the compacted area. This procedure was systematically repeated until an overall height of the soil body of 9.65 m was reached. The relative density, D_r , resulting from the core samples, is shown in Fig. 2 together with the mean value $D_r = 0.736$. The coefficient of variation (COV) defined as the standard deviation divided by the mean value equals 0.027.

As soon as the sand sample was fully assembled, a drainage system was used to allow water to slowly flow (30–40 cm/d) from the bottom of the test pit towards the sand surface. The water level during the experiment was set to 9.15 m (0.5 m below the sand level). The soil sample was further investigated with five CPTs. The layout of the sand pit with CPT and pile locations is shown in Fig. 3. In Fig. 4, the CPT profiles are depicted. It is seen that the profiles match rather good, proving the general uniformity of the prepared volume of sand. Furthermore, the profiles reflect the layered soil preparation where the higher peaks correspond to the most superficial part of each layer, whereas the lower peaks indicate the middle of each sand layer. A reduction in the cone resistance between depths of 6–7 m can also be noted, which is attributed to a slightly thicker sand layer prepared at those depths. However, this

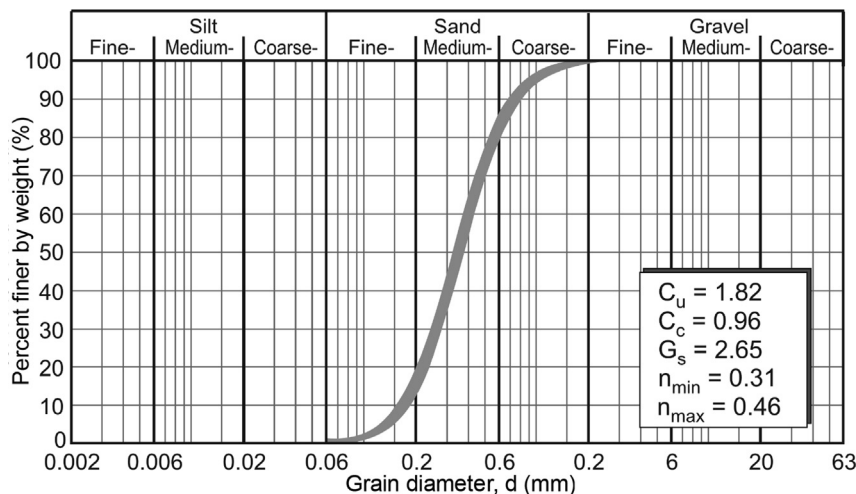


Fig. 1. Grain size distribution of the used sand medium.

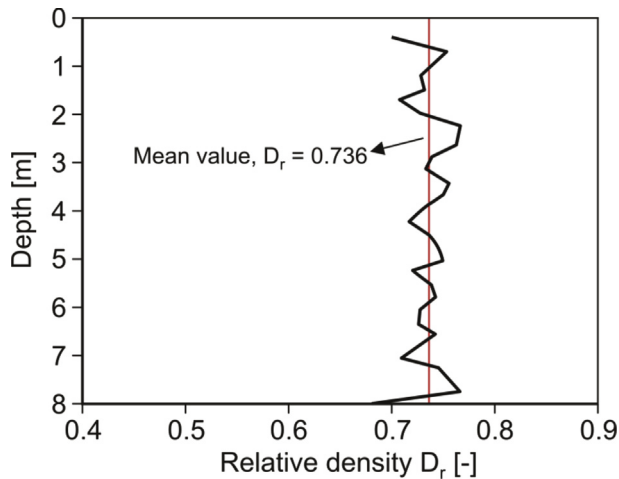


Fig. 2. Relative density over depth of the prepared sand within the test pit.

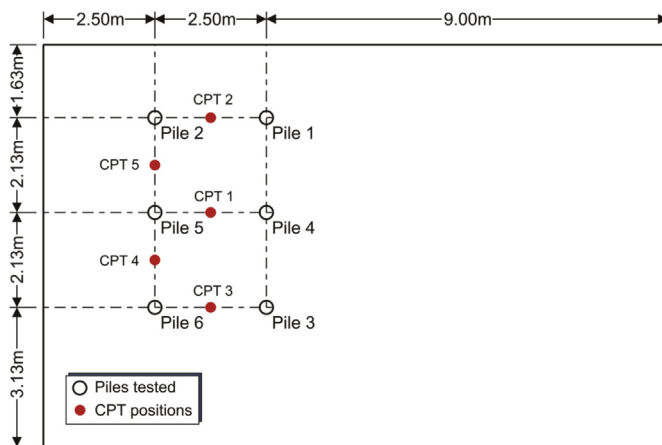


Fig. 3. Layout of the sand pit with pile and CPT positions.

does not have implications for the test campaign, as the trend seems to equally apply to all the investigated points.

2.2. Foundation installation and test execution

The geometries of the tested piles are listed in Table 1, where D is the pile diameter, L is the embedded pile length, and t is the pile wall thickness. The dimensions of the pile sample were appropriately chosen in order to obtain L/D and D/t ratios relevant to research and industry practice. The material of the piles was steel S355 with an average roughness of $10 \mu\text{m}$. On piles 2 and 5, eight strain gages were stuck to the external pile shaft, whereas pile 6 was instrumented with 2 accelerometers protected by two 5 cm-diameter tubes welded to the outer pile shaft. The measurements of these gages and accelerometers were not considered in this paper as the ultimate capacity of the piles and its probabilistic interpretation were the main concerns. Piles 1, 3 and 4 had non-instrumented shafts. The foundations were installed with the impact hammer MENCK SB-120. According to the indications retrieved from foundation standards (e.g. Deutsche Gesellschaft für Geotechnik e.V., 2012), field test studies (e.g. Deeks et al., 2005) and numerical simulations carried out prior to the experiments, a distance of at least $6D$ between the pile axis and border of the sand pit was maintained (see layout in Fig. 3). To support the piles during

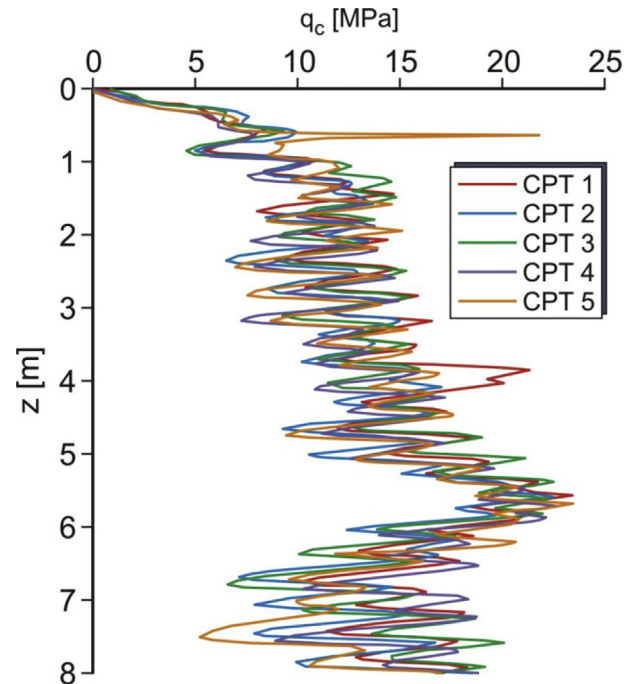


Fig. 4. CPT profiles of the investigated locations in the sand pit according to Fig. 3. q_c is the cone resistance, and z is the depth.

the initial penetration and to ensure verticality throughout the installation process, a pile guide was utilized. A picture of the installation process of pile 2 is depicted in Fig. 5.

To allow plugging, monitoring of the installation was paused after the first three meters of penetration and each meter after that. The ratio of the soil column inside the pile to the embedded pile length, also called plug length ratio (PLR), was on average 0.93 with a COV of 0.02. The number of blows per 10 cm of penetration is shown in Fig. 6. On the whole, the driving resistance seems to reveal the consistent results for various pile geometries, except for piles 4 and 6, where a higher installation resistance had to be overcome compared to piles 3 and 5. Probably this deviation can be linked to the heterogeneity of soil; however, no indication for a higher density can be seen from the CPT profiles.

The time between pile driving and static test was either 35 d or 36 d. The static tests were performed in a displacement-controlled manner with a constant displacement rate of 0.01 mm/s . During the static tests, the displacement of the pile head was measured with a displacement transducer fixed on an independent frame. The piles were tested until a vertical displacement of at least 10% of the diameter was reached. The experimental data were collected by means of a data acquisition system and stored in a computer with a sampling frequency of 10 Hz.

Table 1

List of tested steel piles with appertaining geometry as well as the experimental ultimate capacity.

Pile	D (m)	L (m)	t (mm)	L/D	D/t	Ultimate capacity (kN)
Pile 1 (P1)	0.273	5.7	5	20.9	54.6	157.2
Pile 2 (P2)	0.273	6.7	5	24.5	54.6	123.6
Pile 3 (P3)	0.356	5.7	6.3	16	56.4	187.1
Pile 4 (P4)	0.356	6.7	6.3	18.8	56.4	252.2
Pile 5 (P5)	0.356	5.3	6.3	14.9	56.4	152.8
Pile 6 (P6)	0.356	6.7	6.3	18.8	56.4	219.3

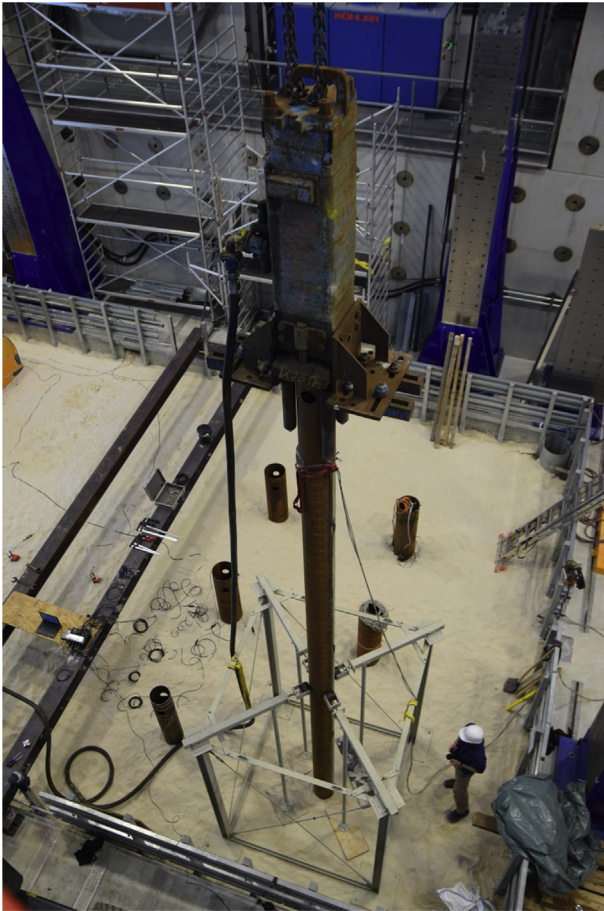


Fig. 5. Pile 2 supported by the pile guide before the pile installation.

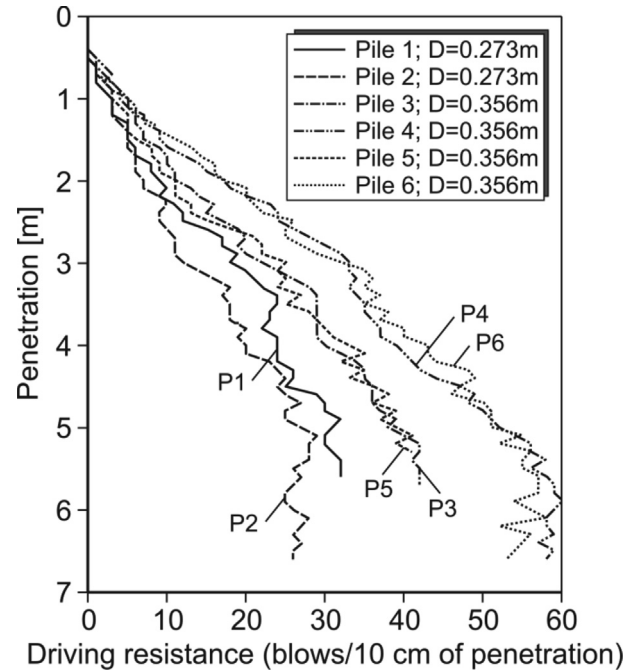


Fig. 6. Driving resistance of all the tested piles.

sensitivity of the loading or to a creep behavior of the pile-soil system.

3. Estimation of model error

3.1. Design methods

Generally it can be observed that the tension load case is the controlling case with regard to the required pile length within the ultimate limit state design for jacket or tripod piles as supports for offshore wind energy converters. Therefore, only tensile capacity is considered here.

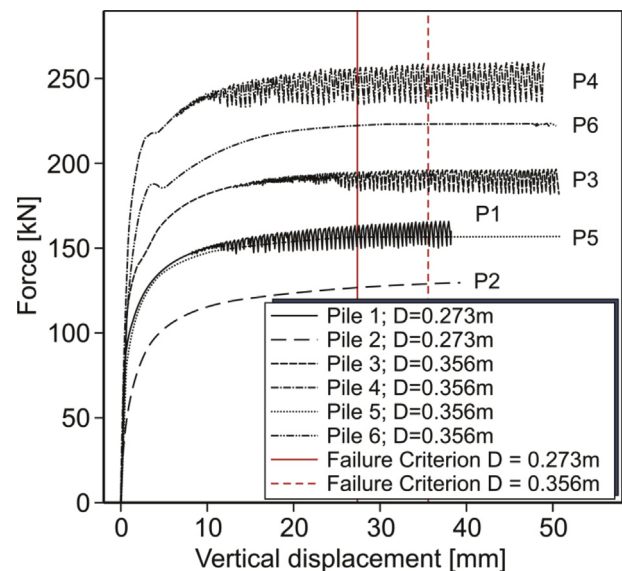


Fig. 7. Load-displacement curves of all tensile tests.

2.3. Experimental results

The experimental curves of all the tests are depicted in Fig. 7. The ultimate capacity was identified according to the well-established 10% diameter criterion (see for instance Deutsche Gesellschaft für Geotechnik e.V., 2012). In Fig. 7, the criteria for the two diameters tested in this experiment series are shown. The ultimate bearing capacity of the piles is listed in Table 1. There appears to be a rather consistent trend between the driving resistances (Fig. 6) and the ultimate capacities obtained.

All the experimental curves present a very high initial stiffness for displacements smaller than 2 mm. After this first substantially elastic part, it is evident that the gradient of the curve starts to decrease tending asymptotically to zero. At 10–20 mm of vertical displacement, an oscillation of the load level with a magnitude of 10%–15% can be noticed for piles 1, 3 and 4. This is related to the high sensitivity of the loading device. By converging towards the ultimate axial bearing resistance of these piles, less additional load must be applied to maintain the prescribed pullout velocity of 0.01 mm/s. Hence, the applied load is reduced to a certain sufficient level. Thereafter an increase in the applied load is required to pull the pile further. However, the upper bound of these load cycles converges to a plausible extension of the load–displacement curves and thus should be taken into account regarding the determination of the capacity.

At 2–5 mm of vertical displacement, an untypical behavior can be observed for piles 4 and 6 in the load–displacement curves. However, it is not clear if this behavior can be related to the

The tensile bearing capacity of an axially loaded pile consists basically of the mobilized friction between the pile outer shaft area and the surrounding subsoil. In practice, the pile effective weight is also taken into account. In case of an open-ended pile, two different conditions of the soil within a pile, namely “plugged” or “unplugged”, must be considered. In the unplugged case, additional resistance due to friction between the pile inner shaft area and the inner soil is assumed. In contrast, for the plugged case, only the unit weight of the inner soil is considered in addition to the resistance. The resulting pile resistances for the two mentioned conditions are given as follows:

$$R_t = \begin{cases} A_o \int f_t(z) dz + G'_s + G_p(\text{plugged}) \\ A_o \int f_t(z) dz + A_i \int f_t(z) dz + G_p(\text{unplugged}) \end{cases} \quad (2)$$

where A_o is the outer pile shaft area, $f_t(z)$ is the skin friction for tension loading, A_i is the inner pile shaft area, G'_s is the effective weight of the inner soil plug, and G_p is the effective weight of the pile.

According to the API Main Text method, in this paper also referred to as API, the minimum of both conditions is decisive and should be considered as the tensile capacity. The skin friction for non-cohesive soil can be determined according to Eq. (3) by multiplying the vertical stress with a β_{API} value, where β_{API} is the shaft friction factor. Further, a limitation of the skin friction is included. Both the shaft friction and the limited friction values only depend on the relative density of the soil. An additional limitation of the tension friction by the factor of 2/3 is not recommended by the API, but this factor is regularly used in practice since it is also prescribed by certification companies like Germanischer Lloyd (2005), owing to the fact that the friction resistance in tension is smaller due to the Poisson’s ratio contraction of the pile shaft and the reduced vertical stresses around the pile compared to the friction resistance in compression. It is not clear if this factor also should be applied to the limited skin friction. However, in this study, the limit skin friction is also reduced according to Eq. (3), which also matches the relation of the friction for tension and compression of the CPT-based methods:

$$f_t(z) = \frac{2}{3} \beta_{API} \sigma'_v \leq \frac{2}{3} f_{t,max} \quad (3)$$

where σ'_v is the effective vertical stress; and $f_{t,max}$ is the limit skin friction, as indicated in Table 2. The values of the shaft friction factor β_{API} are also presented in Table 2.

The determination of the relative density should be done by applying the approach proposed by Jamiolkowski et al. (1988) (see also API, 2007) according to the following equation:

$$D_r = \frac{1}{2.93} \ln \left[\frac{q_c}{205(p'_m)^{0.51}} \right] \quad (4)$$

where q_c is the measured cone tip resistance in kPa, and p'_m is the effective mean in situ soil stress in kPa.

Table 2
Design parameters for the API Main Text method (API, 2007).

Relative density, D_r	β_{API}	$f_{t,max}$ (kPa)
0.35–0.65	0.37	81
0.65–0.85	0.46	96
0.85–1	0.56	115

In contrast to the API Main Text method, the outer skin friction for the CPT-based design methods was correlated directly with CPT measurements. The skin friction for the simplified ICP-05, offshore UWA-05 and Fugro-05 methods can be calculated according to Eq. (5). The friction for the NGI-05 method is given by Eq. (6).

$$f_t(z) = u q_c \left(\frac{\sigma'_v}{p_a} \right)^a A_r^b \left[\max \left(\frac{L-z}{D_o}, \nu \right) \right]^{-c} (\tan \delta_{cv})^d \quad (5)$$

$$f_t(z) = \frac{z}{p_a} \left(\frac{\sigma'_v}{p_a} \right)^{0.25} 2.1 (D_r - 0.1)^{1.7} > 0.1 \sigma'_v \quad (6)$$

where p_a is the atmospheric stress, $p_a = 100$ kPa; $A_r = 1 - (D_i/D_o)^2$ is the pile displacement ratio; D_o is the pile outer diameter; δ_{cv} is the interface friction angle; a, b, c, d, u and ν are the parameters, as listed in Table 3; and the relative density D_r is defined as

$$D_r = 0.4 \ln \frac{q_c}{22 \sqrt{\sigma'_v p_a}} > 0.1 \quad (7)$$

3.2. Reliability of design methods

Several model error approaches regarding the reliability of design methods for axially loaded piles are available in the literature (Jardine et al., 2005; Lehane et al., 2005; Schneider et al., 2008; Achmus and Müller, 2010; Lacasse et al., 2013b). Among them different limitations regarding soil conditions, installation methods and pile specifications are used. A relatively new evaluation of the design methods was presented by Yang et al. (2015), which is based on a new assessed database with in total 80 pile load tests. The used limitations with the corresponding statistical data in terms of the mean and the COV are presented in Table 4. As can be seen, the design methods yield relatively high COVs in between 0.34 and 0.55. Also the mean values deviate from unity by approximately 10%–30%. It should be noticed that only the statistic values of the simplified methods are presented, since these methods are investigated here. The full design approaches of the ICP-05 and UWA-05 methods yield a smaller standard deviation compared to the simplified ICP-05 and offshore UWA-05 methods (Yang et al., 2015).

As mentioned above, the model error strongly depends on the chosen soil, installation and loading conditions, and pile material and geometry. By choosing project-specified boundaries, a more reliable performance of a certain design method can be obtained. By restricting the database only to the tension loaded open-ended steel piles which were impact-driven, statistical values of the model error were presented by Lehane et al. (2005) and Schneider et al. (2008), as listed in Table 4. For both model errors, less deviation in combination with a mean value closer to unity compared to the overall model error proposed by Yang et al. (2015) can be observed.

To cover the usual soil conditions and typically used pile dimensions for wind energy converters in the North Sea (Achmus and Müller, 2010), additional restrictions regarding the density of soil

Table 3
Design parameters for the simplified ICP-05, offshore UWA-05 and Fugro-05 methods (API, 2007).

Method	a	b	c	d	u	ν
Simplified ICP-05	0.1	0.2	0.4	1	0.016	$A_r^{0.25}$
Offshore UWA-05	0	0.3	0.5	1	0.022	2
Fugro-05	0.15	0.42	0.85	0	0.025	$A_r^{0.5}$

Table 4
Model errors for the axial bearing capacity of piles in the literature.

Literature	Limitations	Pile number	Statistic value	API	Simplified ICP-05	Offshore UWA-05	Fugro-05	NGI-05
Yang et al. (2015)	Open- and close-ended, circular and square shape, concrete and steel piles, tension and compression loading	80	μ_{Q_c/Q_m} COV_{Q_c/Q_m}	0.9 0.55	0.7 0.34	0.9 0.4	1.21 0.45	1.23 0.47
Lehane et al. (2005)	Open-ended, steel piles, impact-driven, tension loading	15	μ_{Q_c/Q_m} COV_{Q_c/Q_m}	0.72 0.75	0.9 0.25	0.91 0.23	0.9 0.31	1.01 0.36
Schneider et al. (2008)	Open-ended, steel piles, impact-driven, tension loading	16	μ_{Q_c/Q_m} COV_{Q_c/Q_m}	0.73 0.64	0.96 0.16	0.97 0.19	0.92 0.32	1.04 0.29
Achmus and Müller (2010)	Open-ended, steel piles, impact-driven, tension loading, dense to very dense sand, $L/D = 15-40, D/t = 21-34$	6	μ_{Q_c/Q_m} COV_{Q_c/Q_m}	0.6 0.29	0.88 0.15	0.82 0.14	1.03 0.28	1.15 0.21

^a Geometric mean value.

^b Standard deviation of $\ln(Q_c/Q_m)$.

and the slenderness ratio of a pile were also added. Considering these restrictions, only 6 pile load tests were used (see Table 4). The mean and the COV of the model error are also shown in Table 4. In comparison to both model errors discussed previously, the deviations of the model error obtained by Achmus and Müller (2010) are slightly reduced for all methods. The mean values for the API, simplified ICP-05 and offshore UWA-05 methods are clearly reduced, whereas the mean values for the Fugro-05 and NGI-05 methods are increased.

The model errors for the newly performed pile load tests described above are presented in Table 5. Corresponding to the chosen pile lengths and diameters, the slenderness ratio lies in between 15 and 25. Also the range of the D/t ratio (55–57) is comparable to that of the offshore piles used in the North Sea. It can be noted that the mean values obtained by the simplified ICP-05, offshore UWA-05 and Fugro-05 methods are close to unity, especially when using the simplified ICP-05 method. In contrast, the API method underestimates the axial bearing capacity almost by half, whereas the NGI-05 method overpredicts the capacity by a factor of 2.18. Compared to the model error presented by Achmus and Müller (2010), the deviation is slightly reduced for the CPT-based methods, whereas the deviation for the API Main Text method is reduced almost by half. Regarding the API method, it is known that this method is very conservative, especially in dense sand. On the other hand, the relative high overestimation of the capacity by the NGI-05 method is somewhat surprising. This may be caused by the fact that the NGI-05 method was calibrated based on pile load tests with a relatively small D/t ratio and did not consider the pile wall thickness within the design calculation.

To expand this database of 6 pile load tests, another 6 additional pile load tests mentioned in Achmus and Müller (2010) were reassessed and included in the analysis. The corresponding limitations and statistical values are given in Table 5. The slenderness ratio and the D/t ratio differ considerably. Nevertheless, these ratios are also relevant to industry practice. Since the NGI-05 method obviously does not capture the capacity of the tested piles as described above, only the reassessed pile load tests were

Table 5
Newly derived model errors for the axial bearing capacity of piles.

Source	Limitations	Pile number	Statistic value	API	Simplified ICP-05	Offshore UWA-05	Fugro-05	NGI-05
Piles 1–6 according to Table 1 (this publication)	Open-ended, steel piles, impact-driven, tension loading, dense to very dense sand, $L/D = 15-25, D/t = 55-57$	6	μ_{Q_c/Q_m} COV_{Q_c/Q_m}	0.51 0.19	0.99 0.14	0.93 0.14	1.09 0.15	2.18 0.17
Piles 1–6 (this publication) and reassessed pile tests of Achmus and Müller (2010)	Open-ended, steel piles, impact-driven, tension loading, dense to very dense sand, $L/D = 15-40, D/t = 21-57$	12	μ_{Q_c/Q_m} COV_{Q_c/Q_m}	0.52 0.44	0.94 0.2	0.89 0.19	1.06 0.27	1.23 ^a 0.19 ^a

^a Only reassessed pile load tests from Achmus and Müller (2010) are considered.

considered. As can be seen, the mean values are slightly reduced for the simplified ICP-05, offshore UWA-05 and Fugro-05 methods compared to the model errors related to the tested piles. The mean value for the API method is not significantly changed. Regarding the COV, an increase can be noticed in all cases. For the reassessed NGI-05 method, the mean increases, whereas the COV is almost the same. In other words, the simplified ICP-05 and offshore UWA-05 methods seem to be more suitable for the determination of the tensile capacity compared to the other design methods.

The model errors derived by all the design methods mentioned above were calibrated for a normal and a lognormal distribution by applying Kolmogorov–Smirnov (KS) and Anderson-Darling (AD) tests with a significance level of $\alpha = 5\%$. Table 6 shows the test statistic values (D_n and A^2) and the adjusted critical values for the performed tests. In Table 6, it appears that the API method does not follow a lognormal distribution. For the CPT-based methods, no tested distribution type can be rejected. However, few load tests are available for drawing a reliable conclusion. Since negative values can be excluded for the model error, a lognormal distribution seems to be more suitable for all design methods. In addition, Fig. 8 depicts a $Q-Q$ plot for a lognormal distribution of the model error for the API method in comparison to the simplified ICP-05 method. As can be seen, the deviation is more or less representative.

4. Reliability-based design

4.1. Stochastic subsoil model and simulation

To evaluate the consequences resulting from the obtained reliability of the design methods, probabilistic calculations regarding the corresponding safety as well as the deterministic design were executed. A stochastic model of the pile-soil system was established and used within a Monte-Carlo simulation with 6×10^6 realizations.

The stochastic bearing capacity consists basically of 5 input variables, namely the inherent variability of the cone resistance of a CPT, w_{qc} , the inherent variability of the unit weight, w_{γ} , the

Table 6
Statistics of KS and AD tests for the derived model errors with $\alpha = 5\%$.

Test statistics		API	Simplified ICP-05	Offshore UWA-05	Fugro-05	NGI-05	
KS test	Adjusted critical value	0.242 ^a				0.321 ^b	
	D_n	N	0.154	0.183	0.14	0.17	0.191
		LN	0.265	0.167	0.143	0.184	0.195
AD test	Adjusted critical value	0.648 ^a				0.773 ^b	
	A^2	N	0.297	0.376	0.293	0.412	0.234
		LN	0.9	0.246	0.241	0.317	0.271

^a Number of load test $n = 12$.

^b $n = 6$. N: Normal distribution; LN: Lognormal distribution.

inherent variability of the interface friction angle, $w_{\delta_{cv}}$, the transformation error for the determination of the internal friction angle from the cone resistance of a CPT, $e_{\phi'}$, and a model error, e_R . The load P was directly modeled as an additional input variable representing a 50-year extreme loading event. All used mean values, standard deviations and distribution types are summarized in Table 7. The standard deviations for w_{qc} , $w_{\gamma'}$ and $e_{\phi'}$ were chosen according to the recommendations by Phoon and Kulhawy (1999), whereas the standard deviation for $w_{\delta_{cv}}$ was assumed according to Lacasse et al. (2013a). Regarding the statistics for the load, the recommendations by Holicky et al. (2007) were followed. Due to subsoil genesis, at least two points are used, which are separated from each other, and the soil properties of these two points are more similar. This fact can be taken into account by implying an autocorrelation structure. Hence, an exponential autocorrelation function with an autocorrelation distance of 0.5 m was assumed for the modeled cone resistance of a CPT:

$$\rho(\tau/\theta) = \exp(-\tau/\theta) \tag{8}$$

where ρ is the autocorrelation between two points, τ is the separation distance, and θ is the autocorrelation length.

The autocorrelation structure was implemented by adapting the standard deviation of the cone resistance which was reduced according to the variance reduction theory proposed by Vanmarcke (1977). By doing so, the autocorrelation leads to a reduction of the standard deviation for a property, which has been averaged

over a certain length. Since w_{qc} is valid for the whole pile length, the reduction factor is calculated according to the following equation by taking into account the total embedded pile length in question:

$$\Gamma^2(L_a|\theta) = \left(\frac{\theta}{L_a}\right)^2 \left\{ 2 \left[\frac{L_a}{\theta} - 1 + \exp\left(-\frac{L_a}{\theta}\right) \right] \right\} \tag{9}$$

where Γ^2 is the variance reduction, and L_a is the average length.

According to Simpson (2012), the characteristic values for soil geotechnical parameters were chosen primarily to be about 0.5 times the standard deviation below the mean value in Europe; whereas in the USA, the characteristic values were chosen to be about 0.5–0.75 times the standard deviation below the mean value. Hence, for the deterministic design, the characteristic values for the buoyant unit weight and the interface friction angle were selected to be about 0.5 times the standard deviation below the mean value. On the other hand, the mean value of the cone tip resistance is chosen as the characteristic value, since it corresponds to the usual practice. Concerning the load, the recommendation proposed by Holicky et al. (2007) is applied. This consists of fixed mean value of the load, which should be 0.6 times the characteristic load value. All the used characteristic values are also summarized in Table 7.

For the chosen characteristic load level of 10 MN, a suitable pile diameter of 2 m was selected, as it resembled typical pile dimensions of mainly axially loaded offshore foundation piles. The pile wall thickness was assumed to be constant at 40 mm, which corresponded to a ratio of $D/t = 50$. The axial bearing resistance was calculated by evaluating the corresponding design method with the assumed deterministic and stochastic parameters every 0.2 m. Hence, the dependency of the skin friction on the depth is taken fully into account within the calculations.

4.2. Influence of model error

For the presented design methods and the applied variables, global sensitivity factors or α values were obtained. The α values indicate how the corresponding design method is sensitive to the

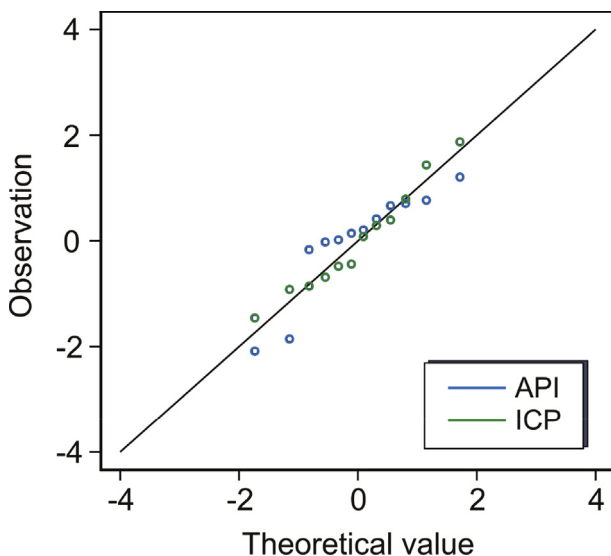


Fig. 8. Q–Q plot for a lognormal distribution of the model error for the API and simplified ICP-05 methods.

Table 7
Assumed statistical properties for the executed deterministic and reliability-based studies.

Variable	Characteristic value	Mean, μ	Standard deviation, σ	Distribution type ^a
w_{qc}	45 MPa	45 MPa	0.4μ	N
$w_{\gamma'}$	9.5 kN/m ³	10 kN/m ³	1 kN/m ³	N
$w_{\delta_{cv}}$	24.2°	26°	3.9°	N
$e_{\phi'}$	–	0	2.8°	N
e_R	–	Database with 12 pile load tests according to Table 5		LN
P	10 MN	6 MN	0.35μ	G

^a Only reassessed pile load tests from Achmus and Müller (2010) are considered. G: Gumbel distribution.

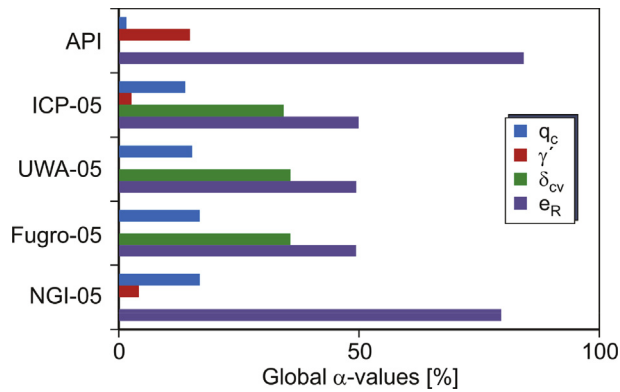


Fig. 9. Global sensitivity values for the investigated design methods and considered input variables.

considered uncertain variables. Basically the α values were calculated by comparing the impact of the input variables on the resistance for one standard deviation above and under the mean value in comparison to that at the mean value (Thurner, 2001). Fig. 9 shows the calculated values for all the mentioned methods. In this figure, the α values are normalized linearly for each design method to 100%.

For the API Main Text method, it can be seen that the model error is the most dominant source of uncertainty in comparison to the soil variables. The variation of the cone resistance almost does not affect the bearing capacity. Consequently, $e_{\phi'}$ does not affect the capacity by any means. Hence, $e_{\phi'}$ is not included in Fig. 9. For the simplified ICP-05 and offshore UWA-05 methods, the model error is almost as dominant as the considered soil uncertainties. Thereby, it is evident that the interface friction angle has almost twice higher influence on the bearing capacity in comparison to the variation in the cone resistance. The uncertainty related to the interface friction angle, which is not directly taken into account by the Fugro-05 and NGI-05 methods, is transferred to the model error. The sensitivity to the cone resistance is in the same range for all the CPT-based methods. Altogether, it can be concluded that the model error represents the most dominant source of uncertainty for the determination of the axial bearing capacity.

4.3. Safety of foundation piles

Firstly a deterministic design was executed by calculating the global safety factor (GSF) for different embedded pile lengths and the assumed characteristic load. The GSF is defined as the ratio of

the characteristic axial bearing resistance R to the load P ($GSF = R/P$). The obtained results are depicted in Fig. 10a. The prescribed partial safety factors in DIN EN 1997 (2009) with national supplementary code DIN 1054 (2010), such as $\gamma_P = 1.35$ for the load and $\gamma_R = 1.5$ for the tension resistance of piles, result in a GSF of 2.03. As can be seen from Fig. 10a, a higher deviation in the required pile length of approximately 25 m arises with respect to different design methods. The CPT-based methods result in a smaller required embedded length, especially the Fugro-05 method, whereas the conservative API method corresponds to the highest required pile length.

By taking into account the stochastic input parameters for the subsoil model and the load, the safety of the pile foundation was determined as a function of the embedded pile length within a Monte-Carlo simulation using 6×10^6 realizations. This is illustrated in Fig. 10b where the safety is expressed in terms of the safety factor β , which is the quantile value of the cumulative standard normal distribution. Hence, the safety factor β can be estimated according to the following relationship:

$$\beta = \Theta^{-1}(1 - p_f) \quad (10)$$

where Θ^{-1} is the inverse of the cumulative distribution function, and p_f is the failure probability.

According to DIN EN 1990 (2010), the safety of offshore foundation piles should correspond to a safety factor of $\beta = 3.8$. Due to the fact that the model error was taken into account, an increase in the required pile length can be observed for all the methods in comparison to the deterministic design. However, a deviation regarding the required embedded pile length still remains. In the case of an ideal model error for each design method, only one safety factor would correspond to a certain depth for each design method, since the model error incorporates the errors within the design method towards the real capacity. Nevertheless, compared to the deterministic design, a deviation in the required pile length has been reduced approximately by half. Thus, the reliability-based method leads to a more robust design. In addition, it is ensured that the required safety margin has been reached. Regarding the interpretation in Fig. 10b, it must be emphasized that only one resistance and thus only one safety factor exist for a certain depth. That means that for a pile length of $L = 38.1$ – 51.1 m, it is required to ensure a safety factor of $\beta = 3.8$ within the considered pile–soil system. On the other hand, it is not possible that a pile with $L = 38.1$ m designed with the simplified ICP-05 method has the same safety factor as a pile with $L = 51.1$ m designed with the API method, although both methods indicate the same safety factor of $\beta = 3.8$ in Fig. 10b for the corresponding lengths.

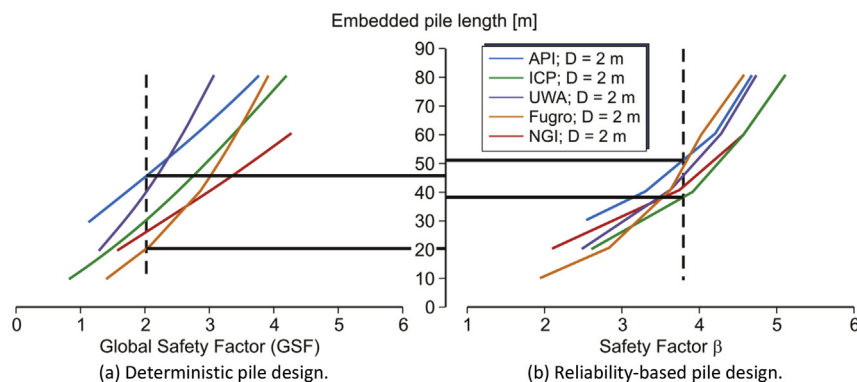


Fig. 10. Global safety factor and β as a function of embedded pile length with respect to different design methods.

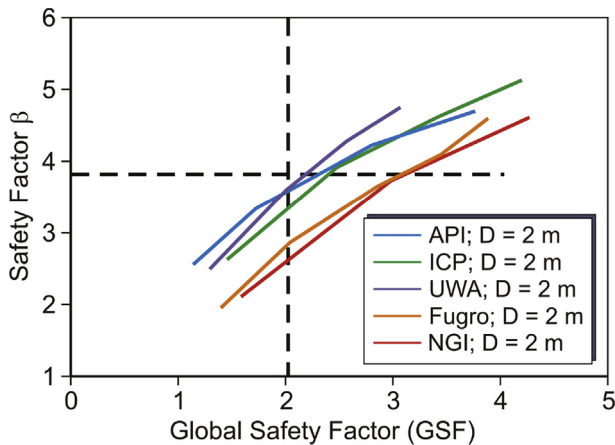


Fig. 11. Safety factor β as a function of the global safety factor with respect to different design methods.

By comparing the results obtained by the deterministic design in terms of GSF and the reliability-based design in terms of the safety factor β in Fig. 11, it can be stated that no deterministic design method leads to the required safety since a GSF of 2.03 should determine a safety factor of $\beta = 3.8$ within the design. This means that the GSF should be in the range of 2.18–3.11 with respect to different design methods. However, these adjusted GSFs are only valid for the corresponding method itself. This means that the application of GSF for $\beta = 3.8$ according to Fig. 11 would lead to the same deviation in the required pile length as indicated in Fig. 10a and consequently to different resistances and safety factors. To avoid these, a more robust and constructive calibration of the GSF has been proposed as follows.

As stated above, only one resistance and one safety factor exist for a certain embedded pile length. From Fig. 10b, it can be seen that for the safety factor of $\beta = 3.8$, the embedded pile length should be at least 38.1 m and preferably not exceed 51.1 m. These lengths can be seen as lower bound (LB) and upper bound (UB) values for $\beta = 3.8$. Based on these lengths, the corresponding GSFs can be estimated for each method. These GSFs represent the required ones for the desired safety factor of $\beta = 3.8$. By doing so, a more robust calibration on the basis of the results of all the reliability-based methods is obtained. Table 8 presents the UB and LB as well as the mean values of the required pile length and the calculated GSFs for the system. Consequently, by assuming a partial safety factor for the load of $\gamma_P = 1.35$, the required partial safety factors for the resistance γ_R can be obtained. The mean value for the required embedded pile length can be seen as the most likely one by taking into account all the design methods. Hence, by relating the calculated mean values of the GSF to the prescribed ones, quality factors for each design method were derived. Thereby a quality factor smaller than unity indicates a conservative design approach. On the

Table 8
Global safety factors and quality factors based on the results of all the reliability-based design methods.

Calibration boundaries	Required pile length, L (m)	Corresponding global safety factor ($\gamma_P \gamma_R$) for P				
		API	Simplified ICP-05	Offshore UWA-05	Fugro-05	NGI-05
LB	38.1	1.6	2.4	1.95	2.75	2.85
UB	51.1	2.31	2.98	2.33	3.15	3.69
Mean	44.6	1.96	2.69	2.14	2.95	3.27
Quality factor (for GSF = 2.03), η		0.97	1.33	1.05	1.45	1.61

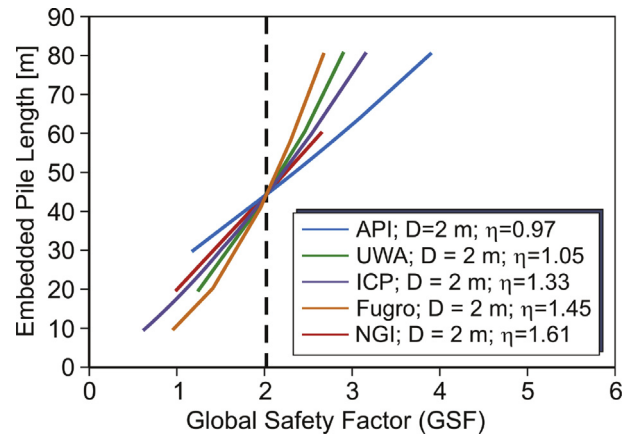


Fig. 12. Outcome of adjusted GSF as a function of the embedded pile length.

other hand, a quality factor higher than unity indicates an overestimation of the capacity by the design method.

Considering the quality factors in Table 8, it can be seen that the prescribed GSF of 2.03 within a deterministic design is sufficient for the API Main Text method, since this method is more conservative in comparison to the other methods (see also Fig. 10a). Also for the conservative offshore UWA-05 method, it can be seen that the quality factor is close to unity. On the other hand, higher quality factors of 1.33, 1.45 and 1.61 were estimated for the simplified ICP-05, Fugro-05 and NGI-05 methods, respectively. This indicates that only for the API method, the current demanded safety and thus the prescribed partial safety factors are valid, whereas for the offshore UWA-05 method, the partial safety factors seem to be in a suitable order. For the simplified ICP-05, Fugro-05 and NGI-05 design methods, the partial safety factor or GSF has to be increased by the quality factor. Same qualitative suggestions regarding the adjustment of the GSF for the API and simplified ICP-05 methods were also reported by Schmoor and Achmus (2013). Considering the corresponding quality factors within a deterministic design, a more robust prediction of the required embedded pile length is possible. Fig. 12 depicts the development of the GSF over the embedded pile length by taking into account the quality factors. As can be seen, all the methods lead to the same embedded pile length of 44.6 m, since this pile length corresponds to the mean value according to the results from all the reliability-based methods (see Fig. 10b).

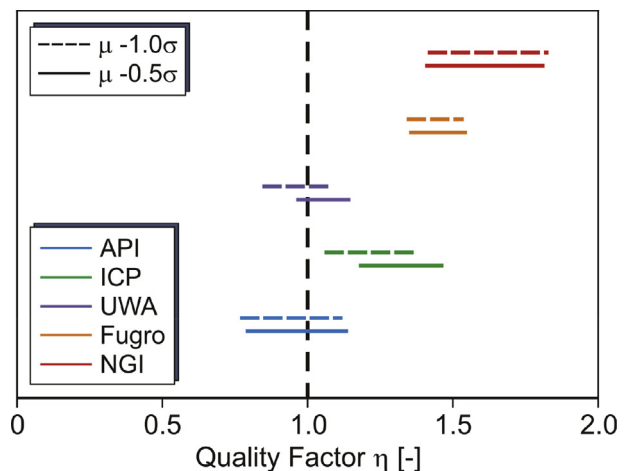


Fig. 13. Influence of the LB and UB values of the required pile length on the corresponding quality factors for two assumptions of the characteristic values.

Comparing to the deterministic design without quality factors, a more robust prediction of the pile capacity has been established, since an adjustment is done by the quality factor for non-conservative methods which tend to overestimate the bearing capacity as well as for conservative methods which tend to underestimate the bearing capacity. However, it should be noted that these calibrated quality factors based on the calculations are only for one dimension of the pile diameter ($D = 2$ m) as well as for one loading condition ($P = 10$ MN). The application of these factors to other diameters or loading conditions may lead to different quality factors.

The choice of the characteristic values for the soil parameters affects the GSF and therefore the quality factors. By choosing a smaller quantile value as a characteristic one for the soil variables, the quality factor decreases, since a more conservative assumption regarding the input properties is made. Fig. 13 depicts the corresponding quality factors for the LB and UB values of the required pile lengths for two assumptions regarding the choice of the characteristic value. In addition to the chosen characteristic value of 0.5 times the standard deviation below the mean value, the corresponding quality factor for a characteristic value of 1 times the standard deviation below the mean value for the buoyant unit weight and the interface friction angle is also shown. A relative large decrease of the quality factor can be seen for the offshore UWA-05 and simplified ICP-05 methods, since these methods are more sensitive to these soil properties compared to the other methods. On the other hand, almost no impact can be observed for the API, NGI-05 and Fugro-05 methods.

5. Conclusions

Six documented axial pile load tests on sand with embedded pile lengths between 5.3 m and 6.7 m, pile wall thicknesses of 5 mm and 6.3 mm, and pile diameters of 0.273 m and 0.356 m were presented. These tests were executed within the IRPWind Project by Fraunhofer IWES.

Five different design methods for the determination of the axial bearing capacity for offshore piles, namely API Main Text, simplified ICP-05, offshore UWA-05, Fugro-05 and NGI-05 methods, were introduced.

On the basis of the measured results, the reliability of the introduced design methods was obtained. Further, these tests were incorporated into a database featuring piles with characteristics relevant to offshore piled foundations used in the North Sea. The data interpretation indicated that the simplified ICP-05 and offshore UWA-05 design methods seem to be more suitable regarding the reliability, whereas the NGI-05 method tends to overpredict the capacity for walled piles ($D/t = 55\text{--}57$). A better prediction of the NGI-05 method can be seen for piles with $D/t = 24\text{--}32$.

A deterministic design using partial safety factors according to DIN EN 1990 (2010) was executed for all methods by assuming typical loading, and pile and soil conditions of the North Sea. Hence, a large deviation in the required pile length can be observed. By assuming typical distribution properties for the soil parameters and the load, and taking into account the newly obtained model errors, the safety factor of the pile foundation was calculated by performing a Monte-Carlo simulation with 6×10^6 realizations. In comparison to the deterministic design, the deviation in the required pile length has been reduced by half, while the required embedded pile length has been increased.

Finally, the consequences of the deterministic design were evaluated. Taking into account the results of reliability-based calculations for all the methods, new GSFs were calibrated for each

design method on the basis of the results of all design methods. The obtained results indicated that the partial safety factors only for the API Main Text method and offshore UWA-05 methods seem to be sufficient with respect to the desired safety level by DIN EN 1990 ($\beta = 3.8$). However, for the simplified ICP-05, Fugro-05 and NGI-05 methods, an increase should be considered.

Conflict of interest

The authors wish to confirm that there are no known conflicts of interest associated with this publication and there has been no significant financial support for this work that could have influenced its outcome.

Acknowledgements

The experimental work and the subsequent data interpretation of this contribution have been carried out as part of the European Union funded project Integrated Research Project Wind (IRPWind, European Union Seventh Framework Program under Grant No. 609795).

References

- Achmus M, Müller M. Evaluation of pile capacity approaches with respect to piles for wind energy foundations in the North Sea. In: Gourvenec S, White DJ, editors. *Frontiers in offshore geotechnics II*. CRC Press; 2010.
- American Petroleum Institute (API). Recommended practice for planning, designing and constructing fixed offshore platforms—Working stress design. API Recommended Practice 2A-WSD (RP2A-WSD). 21st ed 2002. Errata and Supplement 1.
- API. Recommended practice for planning, designing and constructing fixed offshore platforms—Working stress design. API Recommended Practice 2A-WSD. 21st ed 2007. Errata and Supplement 3.
- Deeks AD, White DJ, Bolton MD. A comparison of jacked, driven and bored piles in sand. In: Proceedings of the 16th International conference on soil mechanics and geotechnical engineering (16ICSMGE). Rotterdam, Netherlands: Millpress; 2005. p. 2103–6.
- Deutsche Gesellschaft für Geotechnik e.V. EA-Pfähle. Empfehlungen des Arbeitskreises Pfähle. Berlin: Ernst & Sohn Verlag; 2012 (in German).
- DIN 1054. Baugrund-Sicherheitsnachweise im Erd und Grundbau. Berlin: Deutsches Institut für Normung; 2010 (in German).
- Dithinde M, Phoon KK, De Wet M, Retief JV. Characterization of the model uncertainty in the static pile design formula. *Journal of Geotechnical and Geoenvironmental Engineering* 2011;137(1):70–85.
- DIN EN 1990. Eurocode 0: Grundlagen der Tragwerksplanung. Berlin: Deutsches Institut für Normung; 2010 (in German).
- DIN EN 1997. Eurocode 7: Entwurf, Berechnung und Bemessung in der Geotechnik – Teil 1: Allgemeine Regeln. Berlin: Deutsches Institut für Normung; 2009 (in German).
- Germanischer Lloyd. Rules and guidelines IV, Industrial services: Guideline for the certification of offshore wind turbines. Hamburg, Germany: Germanischer Lloyd; 2005.
- Gilbert RB, Tang WH. Model uncertainty in offshore geotechnical reliability. In: *Offshore technology conference*; 1995. <https://doi.org/10.4043/7757-MS>.
- Holicky M, Markova J, Gulvanessian H. Code calibration allowing for reliability differentiation and production quality. In: Kanda J, Takada T, Furuat H, editors. *Application of statistics and probability in civil engineering: proceedings of the 10th International conference*. London: Taylor & Francis; 2007.
- Jamiolkowski M, Ghionna VN, Lancellotta R, Pasqualini E. New correlations of penetration tests for design practice. In: De Ruiter J, editor. *Penetration Testing 1988: Proceedings of the 1st International Symposium on Penetration Testing (ISOPT-1)*, vol. 1. Rotterdam: A.A. Balkema; 1988. p. 263–96.
- Jardine R, Chow F, Overy R, Standing J. ICP design methods for driven piles in sands and clays. London: Thomas Telford Publishing; 2005.
- Lacasse S, Nadim F, Andersen KH, Knudsen S, Eidsvig UK, Yetginer G, Guttormsen TR, Eide A. Reliability of API, NGI, ICP and Fugro axial pile capacity calculation methods. In: *Offshore technology conference*, Houston, Texas, USA; 2013. <https://doi.org/10.4043/24063-MS>.
- Lacasse S, Nadim F, Langford T, Knudsen Yetginer G, Guttormsen TR, Eide A. Model uncertainty in axial pile capacity methods. In: *Offshore technology conference*, Houston, Texas, USA; 2013. <https://doi.org/10.4043/24066-MS>.
- Lehane BM, Schneider JA, Xu X. CPT based design of driven piles in sand for offshore structures. GEO:05345. University of Western Australia; 2005.
- Phoon KK, Kulhawy FH. Characterization of geotechnical variability. *Canadian Geotechnical Journal* 1999;36(4):612–24.

- Schmoor KA, Achmus M. On the validation of reliability and partial safety factors for axially loaded piles in dense sand. In: Zhang LM, Wang Y, Wang G, Li DQ, editors. Geotechnical safety and risk IV: proceedings of the 4th international symposium on geotechnical safety and risk (4th ISGSR). CRC Press; 2013. p. 455–62.
- Schneider JA, Xu X, Lehane BM. Database assessment of CPT-based design methods for axial capacity of driven piles in siliceous sands. *Journal of Geotechnical and Geoenvironmental Engineering* 2008;134(9):1227–44.
- Simpson B. Eurocode 7: Fundamental issues and some implications for users. Keynote Lecture. Arup Geotechnics; 2012.
- Thurner R. Probabilistische untersuchung in der geotechnik mittels deterministischer finite elemente-methode (PhD Thesis). Institut für Bodenmechanik und Grundbau, Technische Universität Graz; 2001 (in German).
- Vanmarcke EH. Probabilistic modeling of soil profiles. *Journal of the Geotechnical Engineering Division, ASCE* 1977;103(11):1227–46.
- Yang ZX, Jardine RJ, Guo WB, Chow F. A new openly accessible database of tests on piles driven in sands. *Géotechnique Letters* 2015;5(1):12–20.



Dr. Kirill A. Schmoor is present working as Senior Engineer at ACP Prof. Achmus + CRP Planungsgesellschaft für Grundbau mbH, Germany and in the Institute for Geotechnical Engineering at the Leibniz University Hannover, Germany. He obtained his PhD degree from the Leibniz University Hannover, Germany. He has experience in the design of offshore foundation piles including the analysis and interpretation of laboratory tests as well as the application of reliability-based design and evaluation methods. He has worked on more than 15 projects dealing with the design of offshore foundation piles as well as several research projects dealing with reliability-based pile design, and vibratory and rotary-jacking pile installation techniques. He has published research papers in international and national journals and conferences.